Intermediate structural state in $Bi_{1-x}Pr_xFeO_3$ ceramics at the rhombohedral-orthorhombic phase boundary

D. V. Karpinsky [1*], I. O. Troyanchuk [1], M. Willinger [2], V. A. Khomchenko [3], A. N. Salak [4], V. Sikolenko [5], M.V. Silibin [6]

[1] Scientific-Practical Materials Research Centre of NAS of Belarus, P. Brovka str. 19, 220072 Minsk, Belarus

[2] Fritz-Haber-Institut der Max-Planck-Gesellschaft, Abteilung Anorganische Chemie, Faradayweg 4-6, D-14195 Berlin, Germany

[3] CFisUC, Department of Physics, University of Coimbra, P-3004-516 Coimbra, Portugal

[4] Department of Materials and Ceramics Engineering, University of Aveiro, 3810-193 Aveiro, Portugal

[5] Joint Institute for Nuclear Research, 141980 Dubna, Russia

[6]National Research University of Electronic Technology "MIET", 124498 Zelenograd, Moscow, Russia

Abstract

Crystal structure of the $Bi_{1-x}Pr_xFeO_3$ ceramics of the compositions corresponding to the threshold concentrations separating the polar rhombohedral (R3c) and anti-polar orthorhombic (Pbam) phases has been investigated with X-ray diffraction, transmission electron microscopy and differential scanning calorimetry measurements performed in a broad temperature range. The structural study specifies the peculiarities of the temperature-driven transition into the non-polar orthorhombic (Pnma) phase depending on the structural state of the compounds at room temperature. The crystal structure analysis reveals the revival of the anti-polar orthorhombic phase upon the temperature-induced transition, thus assuming that it can be considered as the bridge phase between the polar rhombohedral and the non-polar orthorhombic phases.

Keywords: *Crystal structure, diffraction, intermediate phase, phase transition*

Introduction

Solid solutions of bismuth ferrite attract persistent scientific interest due to the multiple composition-driven structural transitions which dramatically affect the multiferroic behavior. Near the morphotropic phase boundaries, these materials are characterized by the enhanced physical properties associated with the specific structural state. It is assumed that the enhanced responses are caused by a coexistence of the adjacent-phase structural clusters with a typical size reduced down to a nanoscale level. Such structural state is highly defective because of the numerous dislocations, inhomogeneous stress distribution, local variations of the chemical composition etc [1-5] which reduce its thermodynamic stability and enhance sensitivity to the external stimuli – temperature, electric/magnetic field, mechanical stress.

In $BiFeO_3$, chemical replacement of Bi^{3+} with the rare-earth elements possessing comparable ionic radius (La^{3+} - Eu^{3+}) causes the concentration-driven structural transition from the polar rhombohedral to the nonpolar orthorhombic phase that occurs via the formation of the antipolar orthorhombic structure [4, 6-11]. Most promising physical parameters were obtained for the lanthanum and praseodymium-doped compounds within the morphotropic phase boundary region [3, 8, 12], the phase coexistence range estimated for these compounds is stable over a very broad compositional range ($\Delta x \sim 5\%$) far exceeding those attributed to the compounds doped with other rare-earth elements [4, 7]. It should be noted that the wide phase coexistence range facilitates the structural analysis of this region. It is known that the phase transition sequence is largely dependent on the substituting elements, e.g. chemical substitution by rare-earth elements with smaller ionic radii reduces the dopant concentration level triggering the structural transformation, while the width of the phase coexistence region shrinks [4, 13-16].

Structural measurements performed for the rare-earth doped $BiFeO_3$ compounds as a function of temperature have revealed a complex evolution of the structural phases depending on the crystal structure at room temperature [7, 14]. The compounds characterized by the rhombohedral lattice at room temperature demonstrate gradual transition into the non-polar orthorhombic phase that happens via the formation of a mixed (polar + non-polar) structural state. Within the compositional range corresponding to coexistence of the polar and anti-polar phases, a gradual reduction of the anti-polar orthorhombic phase (accompanied by the proportional increase in the amount of the rhombohedral phase) takes place with increasing temperature. At higher temperatures, the anti-polar phase disappears and the new phase with non-polar orthorhombic structure emerges. Further temperature increase stabilizes single phase structural state with the non-polar orthorhombic structure. Ceramics with the major anti-polar phase or single phase anti-polar compounds show gradual transition to the non-polar orthorhombic structure through the two-phase structural state. In the compounds having minority of the rhombohedral phase, anti-polar phase vanishes at temperatures below that attributed to the appearance of the non-polar orthorhombic phase, so such transition is also characterized by two-phase coexistence region without intermediate phases.

Our recent structural study of the Pr-doped compounds [17] within the phase coexistence region has revealed an intriguing evolution of the crystal structure with temperature. The structural measurements performed for the compounds with dominant rhombohedral phase at room temperature show the three-phase coexistent region stable in the narrow temperature range. It was considered that this thermodynamically non-equilibrium state is realized during the temperature-driven transformation of the anti-polar orthorhombic phase into the orthorhombic non-polar phase, while the rhombohedral phase remains notable.

Analysis of the composition- and temperature-driven structural transitions observed in the RE-doped $BiFeO_3$ compounds suggests the anti-polar orthorhombic phase to be the intermediate one between the more stable polar rhombohedral and non-polar orthorhombic phases. The present study focuses on the clarification of the structural evolution of the Pr-doped compounds in the vicinity of the phase boundary region. Analysis of the crystal structure of the compounds across the phase transitions is crucial to determine the origin of the enhanced physical properties observed in these compounds. Declared issue is a complex technological and scientific task as there are different factors which hamper the structural analysis (i.e. limited resolution of laboratory diffractometers, stress and local defects and vacancies which locally modify crystal structure etc.). In order to determine the crystal structure evolution across the phase transitions we have performed the combined microscopic (X-ray diffraction) and local scale (transmission electron microscopy) structural measurements.

Experimental

Ceramic samples of $Bi_{1-x}Pr_xFeO_3$ system with the dopant concentrations $0.1 \leq x \leq 0.25$ were prepared by a two-stage solid-state reaction [4]. High-purity oxides taken in a stoichiometric ratio were thoroughly mixed using a planetary ball mill (Retsch PM 100). The ceramics were synthesized at 930 – 1030°C (synthesis temperature was increased with the praseodymium concentration) followed by a fast cooling down to room temperature. X-ray diffraction measurements were performed with a PANalytical X'Pert MPD PRO diffractometer (Cu-K_α radiation) equipped with a heating stage (Anton Paar, HTK 16N). Diffraction data were analyzed by the Rietveld method using the FullProf software package [18]. High-resolution transmission

electron microscopy (HRTEM) measurements have been performed using an FEI aberration-corrected Titan 80–300 microscope operated at 300 kV equipped with an EDX detector. Differential thermal analysis and differential scanning calorimetry were carried out with a differential scanning calorimeter Setaram (Caluire, France) in a flowing argon atmosphere.

Results and discussion

Crystal structure evolution across the concentration driven transition

XRD measurements performed for the $Bi_{1-x}Pr_xFeO_3$ solid solutions at room temperature have determined the concentration regions specific to different structural phases. The structural data obtained for the compounds with the dopant concentrations of up to x=0.1 were described by the polar rhombohedral phase model (space group *R3c*) specific to the pristine $BiFeO_3$. In the concentration range of $0.11 \leq x \leq 0.15$, the crystal structure of the compounds is characterized by a coexistence of the polar rhombohedral (*R*-phase) and anti-polar orthorhombic (O_2) phases (Fig. 1). The anti-polar orthorhombic structure has been refined using *Pnam* space group with a lattice metric of $\sqrt{2}a_p*2\sqrt{2}a_p*4a_p$ (where a_p is the fundamental perovskite lattice parameter). In the orthorhombic lattice, the ions residing at *A*- and/or *B*- perovskite positions are shifted along the *b*-axis in opposite directions thus forming the anti-polar order similar to that observed in $PbZrO_3$ [19, 20]. Praseodymium doping leads to the increase of the orthorhombic phase fraction at the expense of the rhombohedral one. Quadrupling of the c-axis weakens upon doping and it can hardly be determined in the compounds with x > 0.2. The unit cell is characterized by doubled *c*-axis (as compared to the ideal perovskite structure) and the crystal structure is described by *Pbam* space group with metric $\sqrt{2}a_p*2\sqrt{2}a_p*2a_p$. Increase of the dopant concentration leads to a stabilization of the single phase anti-polar orthorhombic structure (*Pbam*), further chemical doping leads to a stabilization of the two-phase region followed by the single-phase state with the non-polar orthorhombic structure (S.G. *Pbnm*, O_1-phase).

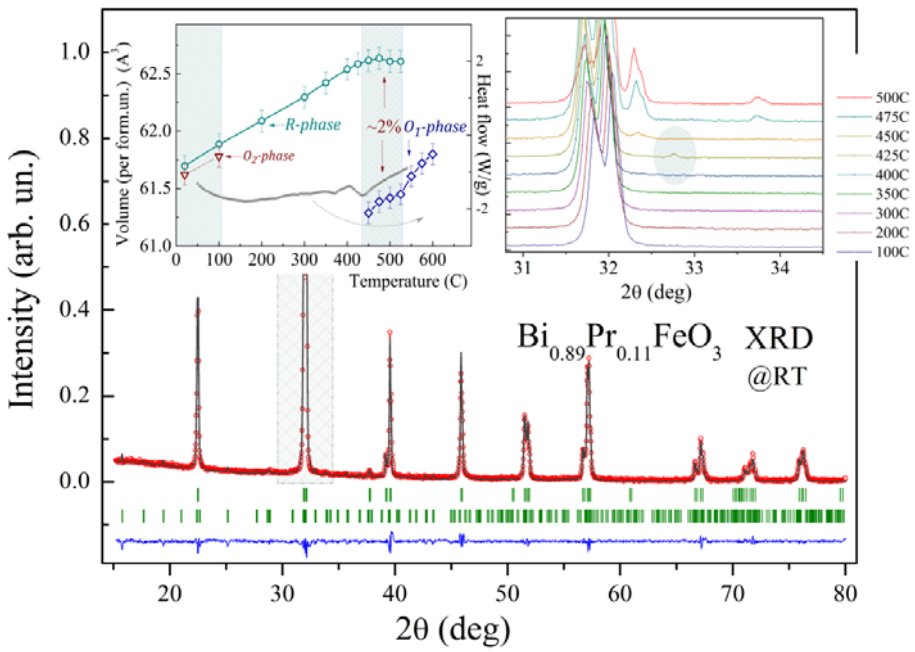

Fig.1. The XRD pattern of the $Bi_{0.89}Pr_{0.11}FeO_3$ compound recorded at room temperature. Bragg positions attributed to the rhombohedral (upper) and the orthorhombic phases are marked by vertical ticks. The right inset shows evolution of the structural peaks, tiny peak attributed to the anti-polar phase is highlighted. The left inset shows temperature evolution of the unit cell volume of the structural phases and the DSC dependence.

The declared structural data generally correspond to the previously published results [17, 21]. Some minor differences with the available data can, however, be found for the two-phase concentration regions and the doping levels critical for the phase transition between the orthorhombic phases. It should be noted that the concentration ranges of the phase stability significantly depend on the synthesis conditions and the post-synthesis treatment (quenching, annealing in gaseous atmospheres etc.). Depending on the mentioned factors, the phase boundary regions can vary within several percents [4, 15, 21, 22]. In the present study we declare ~ 4% width of the rhombohedral-orthorhombic two-phase region which is quite narrow as compared to those reported so far [21, 23].

The anti-polar phase can be considered as the intermediate phase within the structural transition from the rhombohedral to the orthorhombic phase driven by chemical substitution for compounds doped with large rare-earth ions La-Eu; the structural transition in the compounds with smaller dopant ions is associated with direct structural transformation to the non-polar orthorhombic phase. It is known that the concentration of the dopants and the width of the two-phase regions significantly depend on the ionic radius of substituting element. The $BiFeO_3$ compounds doped with lanthanum ions are characterized by smaller changes in the structural parameters upon the chemical doping as compared to those observed in the Pr-doped samples [24], thus justifying a larger concentration of the substituents required to induce the structural transitions as well as a wider range of the two-phase regions.

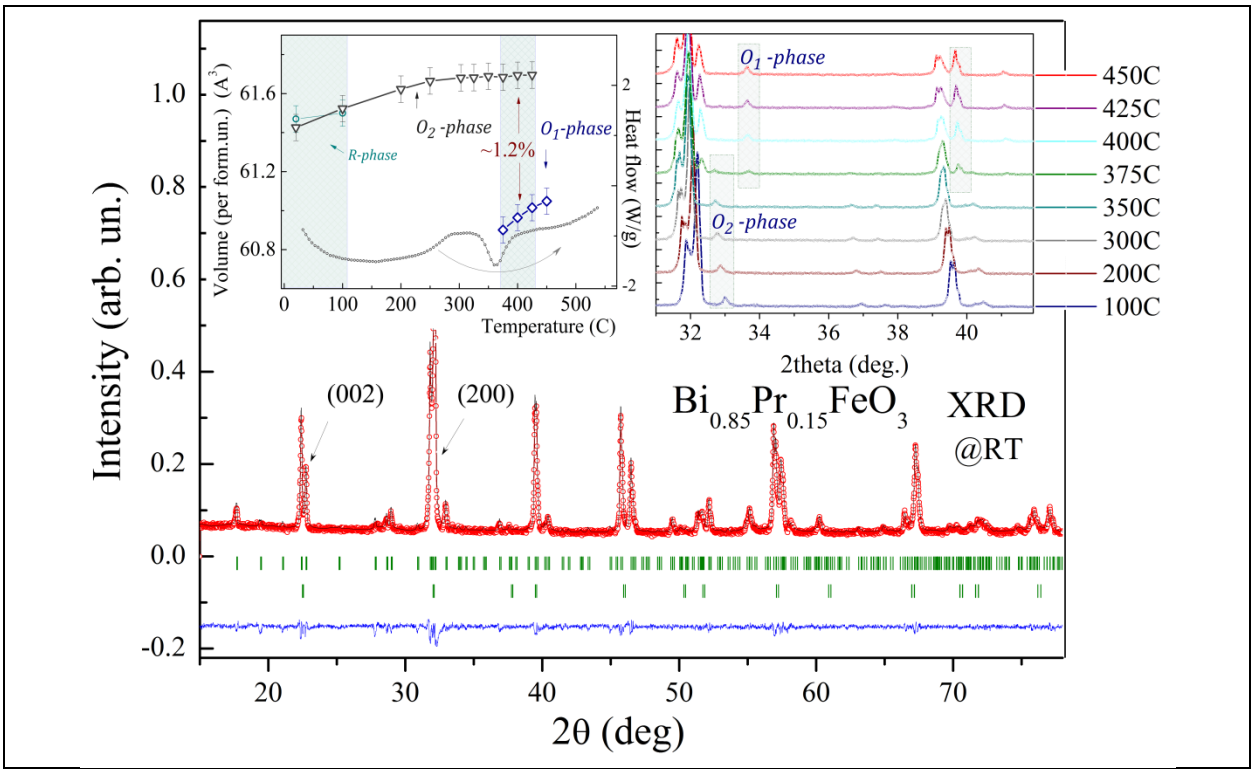

Fig.2. The XRD pattern of the $Bi_{0.85}Pr_{0.15}FeO_3$ compound. Bragg positions attributed to the anti-polar orthorhombic (upper) and the polar rhombohedral phases are marked by vertical ticks. The right inset shows evolution of the structural peaks, the peaks attributed to either anti-polar or non-polar phases are denoted. The left inset shows evolution of the unit cell volume of the structural phases as well as the DSC dependence (solid line).

In contrast, substitution of bismuth ions by rare-earth ions with smaller ionic radii reduces the doping level critical for the structural transition and leads to a shrinkage of the two-phase region [4, 15]. Thus, the size effect plays crucial role in the structural phase transitions observed for the doped $BiFeO_3$ compounds.

Chemical doping with praseodymium ions leads to a gradual reduction of the unit cell parameters. The unit cell volume drastically changes while passing across the phase transitions, viz the rhombohedral-orthorhombic phase transformation is accompanied by ~0.5% change in the unit cell volume, the orthorhombic-orthorhombic transition is accompanied with ~1% change in the unit cell volume. The diffraction data reveal a significant change in the unit cell parameters across the phase transition when the phase ratio evolution testifies a gradual transformation from one phase into the other without any intermediate phase. The crystal structure analysis reveals a minor amount of the anti-polar orthorhombic phase (about 5%) in the compound with x = 11%. The compound with x = 15% is on the other side of the phase boundary and contains about 5% of the rhombohedral phase. The crystal structure of the compound with x=13% is characterized by nearly equal amount of the rhombohedral and the anti-polar orthorhombic phases.

The mentioned compounds represent the doping-driven structural transition from the polar rhombohedral to the anti-polar orthorhombic phase that happens without formation of any intermediate phase. The temperature-driven evolution of the crystal structure resembles that caused by the chemical substitution, while the route of the phase transformation is doubtful and strongly dependent on the initial structural state [14, 24]. The question about the phase coexistence in these compounds upon the temperature increase as well as the possibility of stabilization of the intermediate phase is still under discussion, so the thermal behavior of the compounds within the phase boundary region is worthy to be studied in details.

Temperature driven evolution of the crystal structure

The substitution-driven structural evolution described for the $Bi_{1-x}RE_xFeO_3$ compounds is quite similar to that observed for them upon the temperature increase. The crystal structure of the $Bi_{1-x}RE_xFeO_3$ perovskites transforms into the non-polar orthorhombic one upon the temperature increase regardless the initial structural state stable at room temperature. For the pristine $BiFeO_3$, the rhombohedral-orthorhombic transition occurs at T ~ 830 °C and is accompanied by drastic (~1.5%) decrease in the unit cell volume [25]. The $BiFeO_3$-based compounds doped with different rare-earth ions also show transformation into the non-polar orthorhombic state, while the route of the structural evolution varies for the dopant ions and strongly depends on the structural state at room temperature.

Among the $BiFeO_3$-based materials doped with rare-earth elements, solid solutions with praseodymium ions show the most intriguing evolution of the crystal structure as a function of temperature. For instance, the existence of the three-phase region has been declared for the Pr-doped compounds at temperatures about 380 °C Ref [10], and the authors have justified it in terms of thermodynamically non-equilibrium state. The obtained structural data specify a number of structural transitions occurred in a narrow temperature range as well as the phase coexistence regions. To clarify the percularities of the temperature-driven structural transitions we have thoroughly studied the compounds within the rhombohedral-orthorhombic phase boundary. It should be noted that, in contrast to the La-doped compounds, Pr-containing solid solutions do not show any structural relaxation, thus allowing an accurate study of evolution of their crystal structure.

The detailed structural investigations have been performed for the samples with x=0.11 and x=0.15. The compounds represent nearly entire range of the phase boundary region having

respectively the rhombohedral and the orthorhombic dominant structure at room temperature. The structural data obtained for the former compound demonstrate a fast reduction in the amount of the minor orthorhombic phase and the diffraction peaks attributed to this phase completely disappear at temperatures above 100 °C (Figure 1). The unit cell parameters of the rhombohedral phase show a gradual expansion with increasing temperature up to the temperature of the structural transition into the non-polar orthorhombic phase (T ~ 450 °C). Above this temperature, the unit cell volume remains nearly constant up to the temperature of about 520 °C, where the rhombohedral phase disappears. The unit cell volume calculated for the non-polar orthorhombic phase gradually increases with temperature. The compound is characterized by two-phase coexistence region of about 100 °C. At the temperatures about 450 °C, one can distinguish the traces of the non-polar orthorhombic phase and the crystal structure of the compound becomes single-phase orthorhombic at temperature of about 520 °C; quite narrow temperature region of the two-phase structural state (about 80 °C) testifies the high structural homogeneity of the material.

The compound with x=0.15 is characterized by single-phase anti-polar orthorhombic structure above 100 °C. The additional diffraction peaks observed in the XRD pattern at 375 °C belong to the new structural phase with the non-polar orthorhombic structure (Figure 2, inset). Within the two-phase region, the structural parameters ascribed to the both phases gradually increase and above 430 °C the compound becomes single-phase with the non-polar orthorhombic structure (Figure 2). It should be noted that the variation in the unit cell volume calculated for the compound with x=0.11 is nearly double as compared to that observed for the x=0.15 sample and for the pristine $BiFeO_3$ [25]. The results of differential thermal analysis testify quite small amount of enthalpy associated with this structural transition as compared to those obtained for the pristine compound and for the 15% doped one (Figure 2, inset).

The obtained results indicate a quite complex nature of the structural transition to the non-polar orthorhombic state observed for the compound with x=0.11. Careful analysis of the diffraction patterns at the temperature prior to the formation of the non-polar orthorhombic phase (~ 450°C) allowed the authors to reveal tiny peaks attributed to the anti-polar orthorhombic phase (inset to the Fig. 1, pattern recorded at 425°C for 2theta region about 33 deg.); above this temperature the structure can be successfully refined using the centrosymmetric space group *Pnma*. In order to clarify the observed structural peculiarities, the authors have performed the high resolution transmission electron microscopy measurements (HRTEM).

The HRTEM investigations have been performed in the temperature range 20 – 700°C. The HRTEM images shown in Figure 3 were obtained on a single crystal grain with a size of approximately 100 nm. The FFT images calculated for this region at temperatures above room temperature testify the pattern specific to the rhombohedral phase described by *R3c* space group with (001) zone axis orientation. The FFT image calculated for the temperature of 450°C reveals the appearance of new pair of spots corresponding the plane distances d ≈ 3.9 A in real space and can be associated with (002) reflection attributed to the anti-polar orthorhombic phase (for the compound with x=0.15, the related reflections can be observed at 2theta ≈ 22.7, Figure 2). The FFT performed for the temperature of about ~ 475°C testifies the appearance of new two maximums at d ~ 2.8 (Figure 3), that correspond to (200) reflection which can be observed on the diffraction pattern at 31.7 deg. (Figure 2). The appearance of the non-polar orthorhombic phase detected by HRTEM data explicitly confirms the results of the conventional X-ray diffraction measurements. The spots attributed to the anti-polar orthorhombic structure is observed at temperatures up to 500 °C, further temperature increase leads to a stabilization of the non-polar

orthorhombic structure (the FFT image calculated for the T = 700°C can be successfully simulated using the orthorhombic lattice described by Pbnm space group with (010) zone axis orientation). It should be noted that the X-ray diffraction pattern recorded at T=500 °C has been already refined assuming the singe-phase structural state within the non-polar orthorhombic phase (*Pbnm* space group). The variations in the temperature ranges estimated for the mentioned structural phase can be explained by a difference in the evolution of the crystal structure estimated by microscopic and local scale measurements.

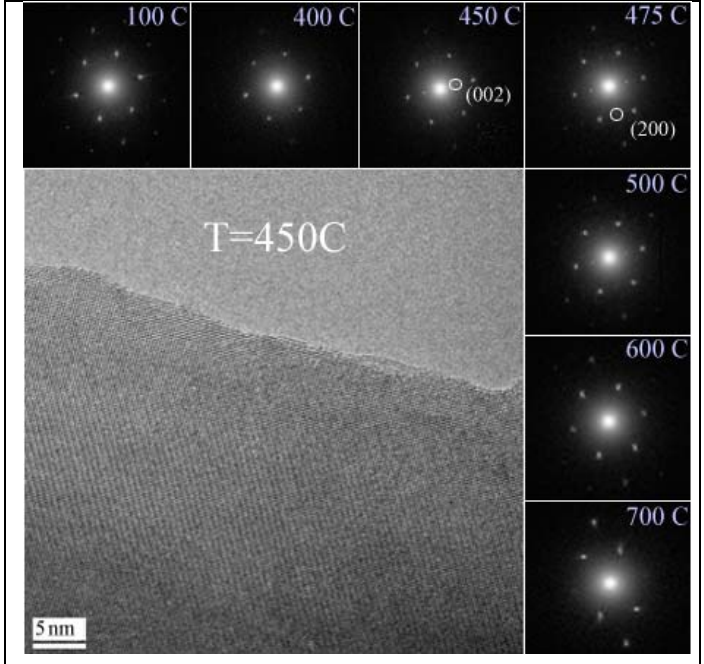

Fig.3. HRTEM image of the compound with x= 0.11 at T= 450°C The insets show FFT images calculated for the temperature region 100 - 700°C.

Conclusions

The temperature- and composition- driven structural transitions in the $Bi_{1-x}Pr_xFeO_3$ ceramics of the compositions within the phase coexistence region have been studied with X-ray diffraction and transmission electron microscopy measurements. The structural analysis have clarified the morphotropic phase boundary region existed in the range of $0.11 \leq x \leq 0.15$ at room temperature. The obtained data have also specified the temperature-driven structural transition into the non-polar orthorhombic phase depending on the initial structural state of the compounds. The structural peculiarities have been followed depending on the phase ratio at room temperature. The structural data have determined a revival of the anti-polar orthorhombic phase with increasing temperature prior to the formation of the non-polar orthorhombic phase. Specific role of the anti-polar phase acting as a mediator between the polar rhombohedral and the non-polar orthorhombic phases across the temperature- and composition driven phase transition has thus been considered.

Acknowledgements

The authors would like to acknowledge the BRFFI (grant F16R-066) RFFI (grant 16-58-00082, 15-58-04009). V.A.K. is grateful to Fundação para a Ciência e a Tecnologia for financial support through the FCT Investigator Programme (project IF/00819/2014). The work done at University of Aveiro was supported by the project TUMOCS. This project has received funding from the European Union's Horizon 2020 research and innovation programme under the Marie Skłodowska-Curie Grant No. 645660.

References

[1] G. L. Yuan, S. W. Or, J. M. Liu, Z.G. Liu, Appl. Phys. Lett., 89 (2006) 052905-052907.
[2] X. Chen, G. Hu, W. Wu, C. Yang, X. Wang, J. Am. Ceram. Soc., 93 (2010) 948-950.
[3] I. O. Troyanchuk, D. V. Karpinsky, M. V. Bushinsky, V. A. Khomchenko, G. N. Kakazei, J. P. Araujo, M. Tovar, V. Sikolenko, V. Efimov, A. L. Kholkin, Phys. Rev. B, 83 (2011) 054109 - 054115.
[4] I. O. Troyanchuk, D. V. Karpinsky, M. V. Bushinsky, O. S. Mantytskaya, N. V. Tereshko, V. N. Shut, J. Am. Ceram. Soc., 94 (2011) 4502-4506.
[5] C.-J. Cheng, D. Kan, V. Anbusathaiah, I. Takeuchi, V. Nagarajan, Appl. Phys. Lett., 97 (2010) 212905.
[6] D. Kan, L. Palova, V. Anbusathaiah, C. J. Cheng, S. Fujino, V. Nagarajan, K. M. Rabe, I. Takeuchi, Adv. Funct. Mater., 20 (2010) 1108-1115.
[7] I. Levin, M. G. Tucker, H. Wu, V. Provenzano, C. L. Dennis, S. Karimi, T. Comyn, T. Stevenson, R. I. Smith, I. M. Reaney, Chem. Mater., 23 (2011) 2166-2175.

[8] D. V. Karpinsky, I. O. Troyanchuk, M. Tovar, V. Sikolenko, V. Efimov, A. L. Kholkin, J. Alloys Compd., 555 (2013) 101-107.
[9] D.V. Karpinsky, I.O. Troyanchuk, M. Tovar, V. Sikolenko, V. Efimov, E. Efimova, V.Y. Shur, A.L. Kholkin, J. Am. Ceram. Soc., 97 (2014) 2631-2638.
[10] D.V. Karpinsky, I.O. Troyanchuk, V. Sikolenko, V. Efimov, E. Efimova, M. Willinger, A.N. Salak, A.L. Kholkin, J Mater Sci, 49 (2014) 6937-6943.
[11] V.A. Khomchenko, I.O. Troyanchuk, M.V. Bushinsky, O.S. Mantytskaya, V. Sikolenko, J.A. Paixão, Materials Letters, 65 (2011) 1970-1972.
[12] D.V. Karpinsky, I.O. Troyanchuk, O.S. Mantytskaja, G.M. Chobot, V.V. Sikolenko, V. Efimov, M. Tovar, Phys. Solid State, 56 (2014) 701-706.
[13] D.V. Karpinsky, I.O. Troyanchuk, A.L. Zheludkevich, O.V. Ignatenko, M.V. Silibin, V.V. Sikolenko, Physics of the Solid State, 58 (2016) 1590-1595.
[14] S. Karimi, I. Reaney, Y. Han, J. Pokorny, I. Sterianou, J. Mater. Sci., 44 (2009) 5102-5112.
[15] D. Arnold, IEEE Trans. Ultrason. Ferroelectr. Freq. Control, 62 (2015) 62-82.
[16] N.V.T. Minh, Dao Viet, J. Nonlinear Opt. Phys. Mater., 19 (2010) 247-254.
[17] D.V. Karpinsky, I.O. Troyanchuk, N.V. Pushkarev, A. Dziaugys, V. Sikolenko, V. Efimov, A.L. Kholkin, J. Alloys Compd., 638 (2015) 429-434.
[18] J. Rodriguez-Carvajal, Physica B, 192 (1993) 55-69.
[19] Rusakov D.A, Abakumov A.M, Yamaura K, Belik A.A, Van Tendeloo G, Takayama-Muromachi E, Chem. Mater., 23 (2010) 285-292.
[20] Teslic S., and Egami T., Acta Cryst. B, 54 (1998) 750-765.
[21] J. Zhang, Y.-J. Wu, X.-J. Chen, Journal of Magnetism and Magnetic Materials, 382 (2015) 1-6.
[22] V. A. Khomchenko, I. O. Troyanchuk, D. V. Karpinsky, J. A. Paixao, J. Mater. Sci., 47 (2012) 1578-1581.
[23] N. Kumar, N. Panwar, B. Gahtori, N. Singh, H. Kishan, V.P.S. Awana, Journal of Alloys and Compounds, 501 (2010) L29-L32.
[24] D. V. Karpinsky, I. O. Troyanchuk, M. Tovar, V. Sikolenko, V. Efimov, E. Efimova, V. Ya. Shur, A. L. Kholkin, J. Am. Ceram. Soc., 97 (2014) 2631-2638.
[25] S.M. Selbach, T. Tybell, M.-A. Einarsrud, T. Grande, Advanced Materials, 20 (2008) 3692-3696.